

## Supporting Information for:

# Kinetic control in the CID-induced elimination of H<sub>3</sub>PO<sub>4</sub> from phosphorylated serine probed by IRMPD spectroscopy.

Francesco Lanucara<sup>\*a</sup>, Barbara Chiavarino<sup>b</sup>, Debora Scuderi<sup>c</sup>, Philippe Maitre<sup>c</sup>, Simonetta Fornarini<sup>b</sup> and Maria Elisa Crestoni<sup>\*b</sup>

<sup>a</sup>Manchester Institute of Biotechnology, School of Chemistry, University of Manchester 131 Princess Street, M17DN Manchester (UK).

<sup>b</sup>Dipartimento di Chimica e Tecnologie del Farmaco, La Sapienza Università di Roma, P.le Aldo Moro 5, 00185 Roma (Italy).

<sup>c</sup>Université Paris Sud, Laboratoire de Chimie Physique, UMR8000 CNRS Faculté des Sciences, Bâtiment 350, 91405 Orsay Cedex (France).

\*Corresponding authors :

Francesco Lanucara Tel. (+44) 161 306 4586/4821

Email address: [francesco.lanucara@manchester.ac.uk](mailto:francesco.lanucara@manchester.ac.uk)

Maria Elisa Crestoni Tel. (+33) 06 4991 3596/3878

Email address : [mariaelisa.crestoni@uniroma1.it](mailto:mariaelisa.crestoni@uniroma1.it)

## Contents :

### - Experimental Methods.

- **Computational Details.** Any additional computational detail and material (xyz files of computed structures, calculated vibrational frequencies for all structures, etc.) is available upon request.

### - References

- **Figure S1.** Photodissociation mass spectrum of C<sub>3</sub>H<sub>6</sub>NO<sub>2</sub><sup>+</sup> ions at *m/z* 88 before (bottom trace) and after (upper trace) irradiation with CLIO FEL IR frequency fixed at 1200 cm<sup>-1</sup>.

- **Figure S2.** CID breakdown graph of C<sub>3</sub>H<sub>6</sub>NO<sub>2</sub><sup>+</sup> ions at *m/z* 88 (●) to afford ions at *m/z* 70 (□) and 42 (○).

- **Figure S3.** Optimized geometries of C<sub>3</sub>H<sub>6</sub>NO<sub>2</sub><sup>+</sup> isomers **1, 2, 3, 4, 5, 6, 7, 8**, obtained at the B3LYP/cc-pVTZ level of theory.

- **Figure S4.** IRMPD spectrum of C<sub>3</sub>H<sub>6</sub>NO<sub>2</sub><sup>+</sup> ions at *m/z* 88 and calculated IR spectra of optimized structures **2, 5, 6, 7, 8**.

- **Table S1.** Thermodynamic data for the lowest energy structures of C<sub>3</sub>H<sub>6</sub>NO<sub>2</sub><sup>+</sup>, calculated at the B3LYP/cc- pVTZ level of theory.

## Experimental Methods

Protonated phosphorylated serine (pSerH)<sup>+</sup> at  $m/z$  186 was obtained by direct infusion of a 10  $\mu\text{M}$  H<sub>2</sub>O/MeOH (1:1) solution of pSer through a fused-silica capillary to the electrospray ionization (ESI) source by a syringe pump at a typical flow rate of 3  $\mu\text{L min}^{-1}$ . When this species was subjected to low-energy collision-induced dissociation (CID) using either a Fourier Transform ion cyclotron resonance (FT-ICR) or a Paul-type ion trap (Bruker Esquire 6000+) mass spectrometer, the formation of the C<sub>3</sub>H<sub>6</sub>NO<sub>2</sub><sup>+</sup> fragment ion ( $m/z$  88) by H<sub>3</sub>PO<sub>4</sub> loss is observed.

Energy variable Collision Induced Dissociation (CID) experiments have been carried out in a commercial hybrid triple quadrupole linear ion trap mass spectrometer (2000 Q-TRAP, Applied Biosystem), holding a Q1q2Q<sub>LIT</sub> configuration (Q1: first mass analyzing quadrupole, q2: nitrogen filled collision cell, Q<sub>LIT</sub>: linear ion trap). The sampled C<sub>3</sub>H<sub>6</sub>NO<sub>2</sub><sup>+</sup> ion, obtained upon in source CID of electrosprayed (pSerH)<sup>+</sup>, was mass selected in Q1 and allowed to collide with N<sub>2</sub> (nominal pressure of 3.2 x 10<sup>-5</sup> mbar) in the quadrupole collision cell q2 at variable collision energies ( $E_{\text{lab}} = 5\text{-}50$  V) for CID experiments. The ionic products were monitored by scanning Q<sub>LIT</sub> in the enhanced operation mode in order to increase both the signal intensity and the resolution. Quantitative threshold values are not directly accessible. Nevertheless, when the relative abundances of fragment ions are plotted as a function of the collision energy, converted to the center of mass frame ( $E_{\text{CM}} = [m/(m + M)]E_{\text{lab}}$ , where  $m$  and  $M$  are the masses of the collision gas and of the ion, respectively), breakdown curves modelled by a sigmoid function can be gained. Extrapolation of phenomenological threshold energies (TE) of the various fragmentation channels can thus be derived, which allows a comparative analysis among competitive dissociation pathways.<sup>1</sup>

As shown in Figure S2, the dissociation process prevailing at lower collision energies (TE = 164 ± 29 kJ mol<sup>-1</sup>) yields an ion at  $m/z$  70, formed by cleavage of water. At higher collision energies (TE = 265 ± 46 kJ mol<sup>-1</sup>) a secondary fragmentation becomes predominant leading to ions at  $m/z$  42, implying further loss of CO from ions at  $m/z$  70. Although this treatment does not provide a direct measure of the threshold energy for dissociation, it indicates dehydration of C<sub>3</sub>H<sub>6</sub>NO<sub>2</sub><sup>+</sup> as the lowest energy fragmentation route.

IR spectroscopy of mass-selected C<sub>3</sub>H<sub>6</sub>NO<sub>2</sub><sup>+</sup> ions was performed employing two experimental setups. The mid-IR range (940-1900 cm<sup>-1</sup>) was explored using the bright and tunable IR radiation of the FEL beamline at the Centre Laser Infrarouge d'Orsay (CLIO) coupled to a modified commercial 7T FT-ICR mass spectrometer (Bruker, Apex Qe), equipped with an Apollo II ESI source.<sup>2</sup> Following mass selection of (pSerH)<sup>+</sup> using a quadrupole mass filter, C<sub>3</sub>H<sub>6</sub>NO<sub>2</sub><sup>+</sup> ions were obtained by CID in a linear hexapole ion trap pressurized with Ar (at ca. 10<sup>-3</sup> mbar), and then extracted and sent to the ICR cell where they were mass selected, trapped at a background pressure of about 1.5 x 10<sup>-10</sup> mbar, and then exposed to IR FEL light for 1 s. In the present case, the sampled ions were irradiated by a 36 ms long CO<sub>2</sub> laser pulse (BFI Optilas, Evry, France) following each CLIO-FEL pulse with a delay of a few  $\mu\text{s}$ . The FEL radiation is based on a 10–48 MeV electron linear accelerator, and is delivered in 8  $\mu\text{s}$  macropulses, at 25 Hz. Each macropulse consists of a train of 500 micropulses (few picoseconds long) and typical macropulse energy is 40 mJ. For the present study, the electron energy was set to 44.4 MeV with an average laser power changing from 900 to 650 mW upon increasing wavenumber. The IR-FEL spectral width (fwhm) was less than 0.5% of the central wavelength.

The 3140-3700 cm<sup>-1</sup> wavenumber region has been investigated using an Optical Parametric Oscillator/Amplifier (OPO/OPA from LaserVision, Bellevue, WA, USA) laser system, coupled to a modified Paul-type ion trap mass spectrometer (Bruker Esquire 6000+) [4]. The parametric converter is pumped by an Nd:YAG laser (Continuum Surelite II) operating at 10 Hz repetition rate and delivering 600 mJ/pulse (each pulse 4-6 ns long). In the investigated spectral range, the typical

output pulse energy from the OPO/OPA laser source was 20 mJ/pulse, with a spectral bandwidth of about 3-4  $\text{cm}^{-1}$ . In the ion trap the ions were accumulated for 20 ms, and typically irradiated for 2 s. When the IR light is in resonance with an active vibrational mode of the sampled ion, several events of photon absorption and intramolecular vibrational energy redistribution can ultimately lead to the fragmentation of the mass-selected species. In both the explored regions, the dissociation channel observed upon irradiation of  $\text{C}_3\text{H}_6\text{NO}_2^+$  ( $m/z$  88) at active wavelengths yields a fragment ion at  $m/z$  70 by loss of  $\text{H}_2\text{O}$ , which in turn dissociates to the ionic species at  $m/z$  42 and neutral CO only in the case of highly active vibrational resonances.

According to the estimated  $164 \pm 29 \text{ kJ mol}^{-1}\text{TE}$  value, the primary photofragmentation process clearly requires the absorption of multiple (more than 3) photons even in the short wavelength range (3140–3700  $\text{cm}^{-1}$ ), where the photon energy is 38–44  $\text{kJ mol}^{-1}$ .

By recording the photofragmentation yield  $R$  (defined as  $R = -\ln(I_{\text{parent}}/(I_{\text{parent}} + \sum I_{\text{fragment}}))$  where  $I_{\text{parent}}$  is the parent ion intensity and  $\sum I_{\text{fragment}}$  is the sum of the intensities of all photofragment ions) as a function of the IR wavenumber, an IRMPD spectrum is obtained. At each spectral point three mass spectra were recorded and averaged.

### Computational details

Density functional theory (DFT) calculations were performed at the B3LYP/cc-pVTZ level of theory to obtain the geometries, energetics and linear IR spectra of low-lying structures of the sampled  $\text{C}_3\text{H}_6\text{NO}_2^+$  ion. All calculations were carried out using the Spartan 10 software package. The optimized structures were subjected to harmonic frequency analysis to characterize the stationary points as local minima. The relative energies at 0 K, were evaluated for each conformer. Enthalpies and free energies at 298 K have been calculated using zero point energy (ZPE) and thermal corrections obtained from unscaled harmonic frequencies.

In order to obtain IR spectra to be compared with the experimental IRMPD spectra, the calculated harmonic vibrational frequencies were scaled by a factor of 0.973 (0.960) in the 940–1900  $\text{cm}^{-1}$  (3140–3700  $\text{cm}^{-1}$ ) spectral region, on the basis of the good agreement between the experimental and computed frequencies. Theoretical IR stick spectra were convoluted with a gaussian profile with an associated width (FWHM) of 20  $\text{cm}^{-1}$  (5  $\text{cm}^{-1}$ ) in the 940–1900  $\text{cm}^{-1}$  (3140–3700  $\text{cm}^{-1}$ ) frequency range for consistency with the experimental spectral resolution.

Additionally, calculations using a larger basis set, namely at B3LYP/6-311++G(2df,2p) level, were performed in order to evaluate whether a better agreement between the observed and theoretically predicted vibrational modes for structure (3) could be obtained. It was found that the same scaling factors of 0.973 and 0.960 for the 940-1900  $\text{cm}^{-1}$  and 3140-3700  $\text{cm}^{-1}$  ranges, respectively, had to be applied for comparing the theoretical and experimental IR spectra.

### References

- 1 (a) P. Milko, J. Roithova, D. Schroeder, J. Lemaire, H. Schwarz and M. C. Holthausen, *Chem.–Eur. J.* 2008, **14**, 4318–4327; (b) G. Bouchoux, J. Y. Salpin and D. Leblanc, *Int. J. Mass Spectrom. Ion Processes* 1996, **153**, 37–48.
- 2 J. M. Bakker, T. Besson, J. Lemaire, D. Scuderi and P. Maitre, *J. Phys. Chem. A*, 2007, **111**, 13415–13424.
- 3 R. K. Sinha, U. Erlekam, B. J. Bythell, B. Paizs and P. Maitre, *J. Am. Soc. Mass Spectrom.*, 2011, **22**, 1645–1650.
- 4 R. K. Sinha, P. Maitre, S. Piccirillo, B. Chiavarino, M. E. Crestoni and S. Fornarini, *Phys. Chem. Chem. Phys.*, 2010, **12**, 9794–9800.

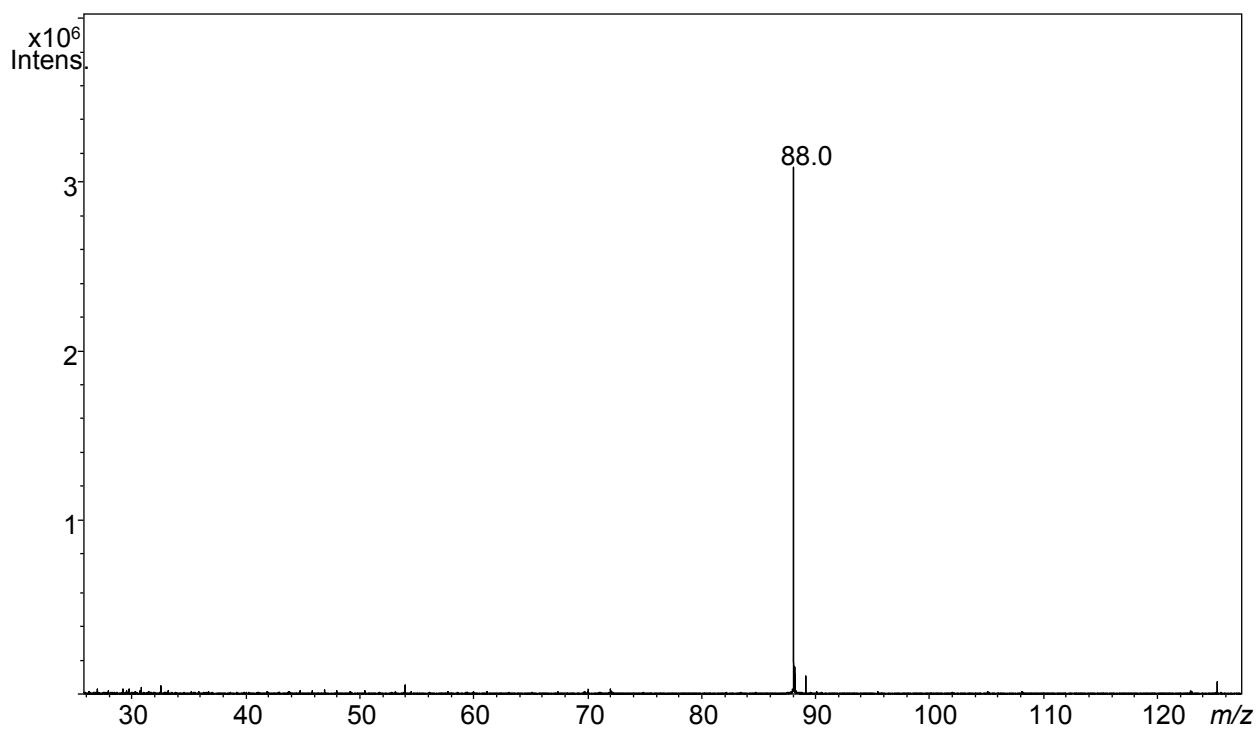
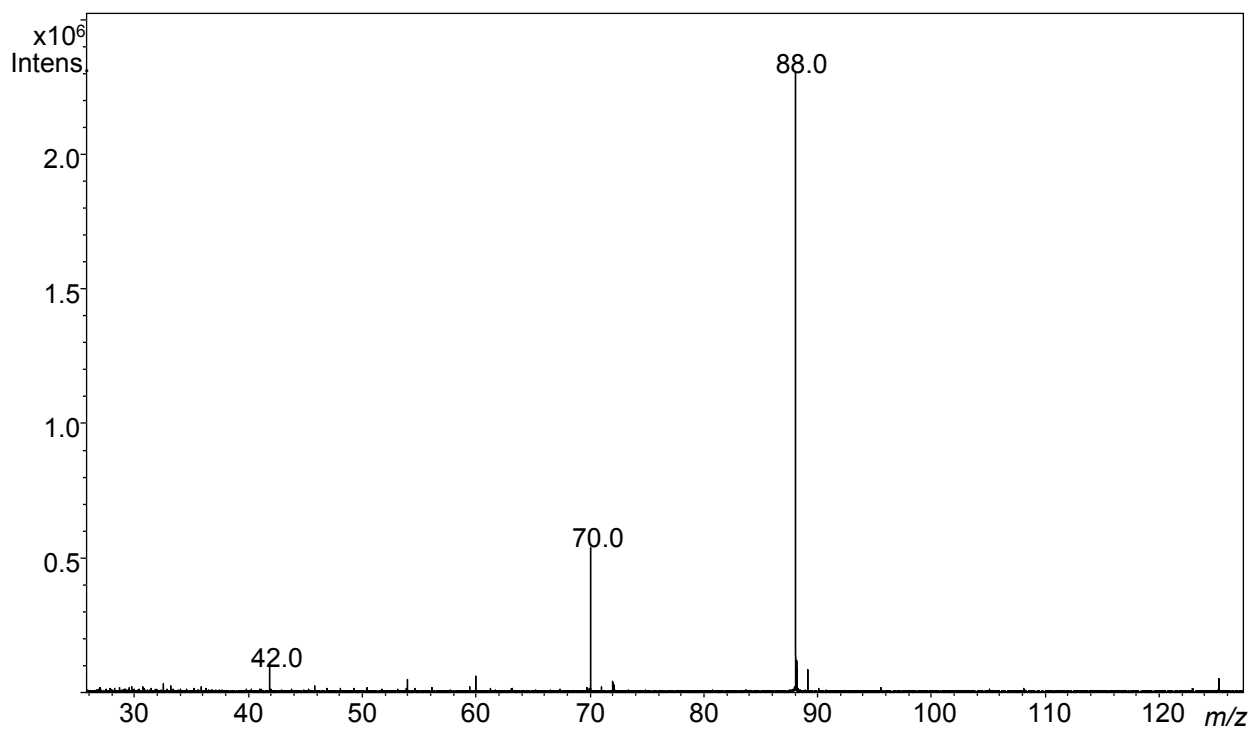


**Figure S1.** Photodissociation mass spectrum of  $C_3H_6NO_2^+$  ions at  $m/z$  88 before (bottom trace) and after (upper trace) irradiation with CLIO FEL IR frequency fixed at  $1200\text{ cm}^{-1}$ .

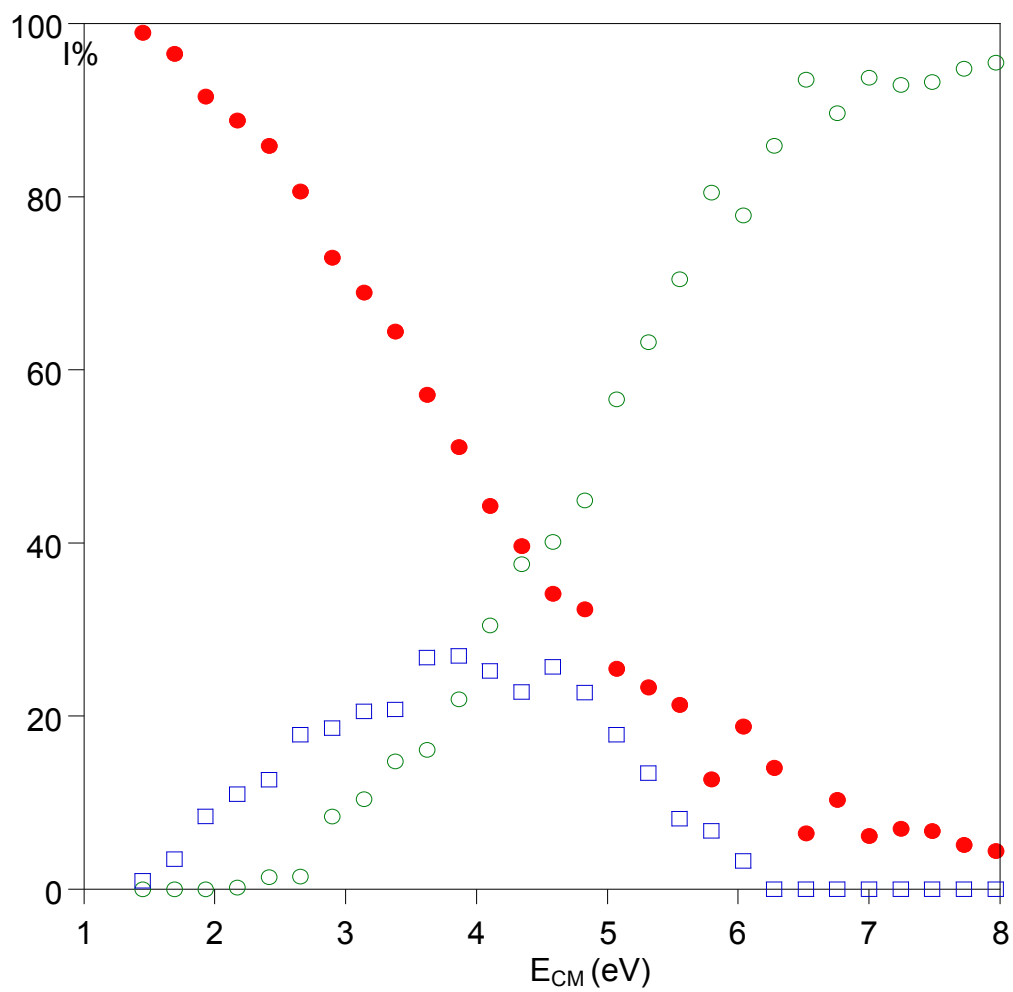


**Figure S2.** CID breakdown graph of  $C_3H_6NO_2^+$  ions at  $m/z$  88 (●) to afford ions at  $m/z$  70 (□) and 42 (○).

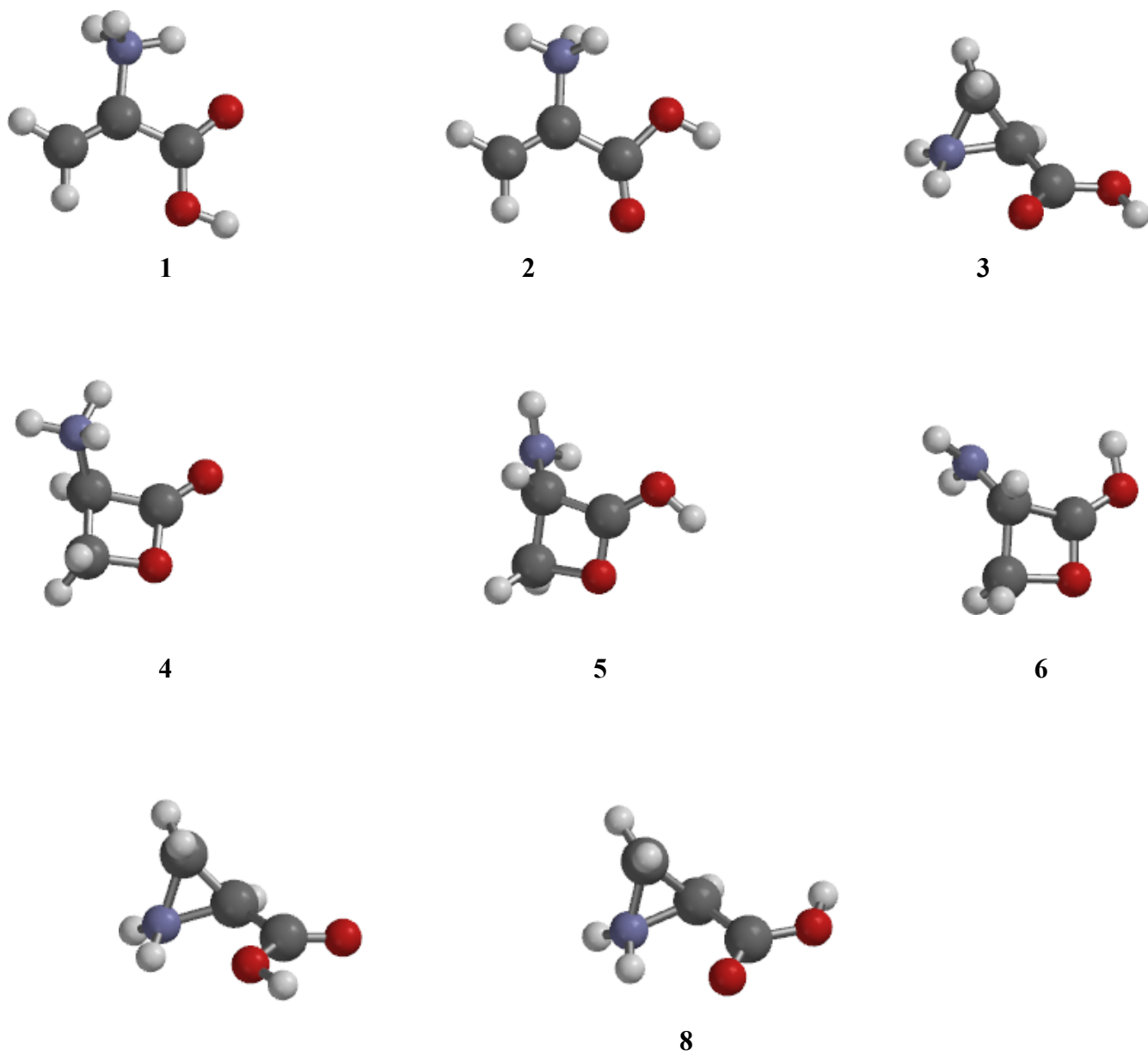


**Figure S3.** Optimized geometries of C<sub>3</sub>H<sub>6</sub>NO<sub>2</sub><sup>+</sup> isomers 1, 2, 3, 4, 5, 6, 7, 8, obtained at the B3LYP/cc-pVTZ level of theory.

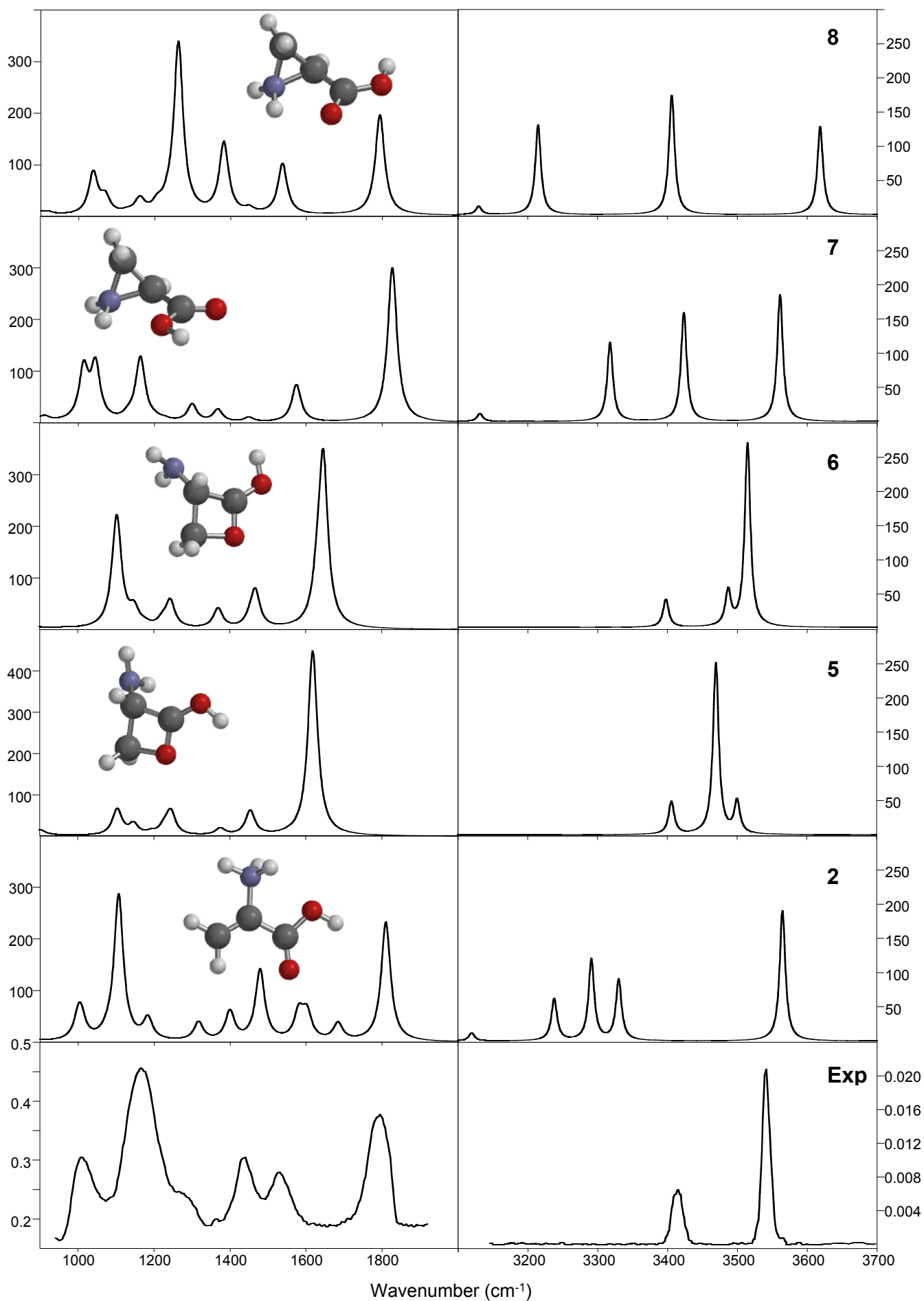


**Figure S4.** IRMPD spectrum of  $C_3H_6NO_2^+$  ions at  $m/z$  88 and calculated IR spectra of optimized structures 2, 5, 6, 7,

**TABLE S1**

Thermodynamic data for the lowest energy structures of  $C_3H_6NO_2^+$ , calculated at the B3LYP/cc-pVTZ level of theory.

Species	$E^a$	$\Delta E_{\text{rel}}$	ZPE <sup>b</sup>	$\Delta H_{\text{rel}}^\circ{}^b$	$\Delta G_{\text{rel}}^\circ{}^b$
<b>1<sup>c</sup></b>	-322.997487	0	276.1	0	0
<b>2<sup>d</sup></b>	-322.989738	2.6	275.4	19.6	19.5
<b>3<sup>c</sup></b>	-322.979121	48.2	277.1	49.2	52.3
<b>7<sup>d</sup></b>	-322.973077	64.1	276.8	64.8	67.3
<b>8<sup>d</sup></b>	-322.966446	81.5	276.5	81.9	84.9
<b>4<sup>c</sup></b>	-322.958908	101.3	279.3	104.4	106.5
<b>5<sup>d</sup></b>	-322.945569	136.3	273.9	134.1	135.9
<b>6<sup>d</sup></b>	-322.945357	136.8	274.7	135.4	137.5

<sup>a</sup>Electronic energy at 0 K in Hartree particle<sup>-1</sup>.

<sup>b</sup>Zero point energies (ZPE), relative enthalpies ( $\Delta H_{\text{rel}}^\circ$ ), and Gibbs free energies ( $\Delta G_{\text{rel}}^\circ$ ) at 298 K in kJ mol<sup>-1</sup>.

<sup>c</sup>Optimized structures depicted in Figures 1 and S3.

<sup>d</sup>Optimized structures depicted in Figures S3 and S4.